Springer

KSME

Journal of Mechanical Science and Technology 32 (3) (2018) 1171~1180
www.springerlink.com/content/1738-494x(Print)/1976-3824(Online)
DOI 10.1007/s12206-018-0220-y

Design optimization of mixed-flow pump impellers with various shaft diameters at the same specific speed†

Sung Kim[1,2], Ung-Been Jeong[1,2], Kyoung-Yong Lee[1], Jin-Hyuk Kim[1], Joon-Yong Yoon[2] and Young-Seok Choi[1,*]

[1]*Thermal & Fluid System R&D Group, Korea Institute of Industrial Technology, 89 Yangdaegiro-gil, Ipjang-myeon, Seobuk-gu, Cheonan-si, Chungcheongnam-do 31056, Korea*
[2]*Department of Mechanical Design Engineering, Graduate School, Hanyang University, 222 Wangsimri-ro, Seongdong-gu, Seoul 04763, Korea*

(Manuscript Received July 21, 2017; Revised November 28, 2017; Accepted December 11, 2017)

Abstract

In this study, the hydraulic performance of a mixed-flow pump depending on the impeller hub ratio was analyzed using Computational-fluid-dynamics (CFD). The impeller inlet shape varies according to the hub ratio even at the same specific speed. It is important to ensure an optimum impeller design according to the hub ratio in order for the impeller shape to provide the desired performance at constant specific speed. The design variables of inlet part for meridional plane and vane plane development were defined for optimum impeller design. The objective functions were defined as the total head and total efficiency of the mixed-flow pump impellers. The optimum impeller design was carried out by controlling the design variables of impeller inlet parts by using the Response-surface-method (RSM). The tendency of impeller design variables depending on the hub ratio was identified by analyzing the optimum impeller design. Further, the impeller shape was designed on the basis of the tendency of the design variables depending on the hub ratio. Finally, the performance of an impeller with the designed shape was verified by numerical analysis.

Keywords: Mixed-flow pump; Impeller; Hub ratio; Design optimization; Computational fluid dynamics (CFD); Response surface method (RSM)

1. Introduction

The mixed-flow pump is fluid machinery that is widely used in many industries as well as domestically. Even though it is used in many different industries already, further researches aiming increase of energy efficiency are essential due to its enormous energy consumption. Therefore, pump designing for performance improvement is getting more important and it takes experience and theory to design a pump with improved performance.

The mixed-flow pump is used in various industries and has numerous applications. Therefore, its design specifications such as design flow rate, total head, and rotational speed need to be varied, even at the same specific speed. Thus, various impeller designs are required. In particular, as the pump size increases, the size of the shaft diameter also increases, even at the same specific speed. Thus, a larger hub ratio is required on the impeller meridional plane. As the impeller inlet shape varies according to the hub ratio, the impeller of a mixed-flow pump needs to be redesigned while considering the hub ratio in order to obtain the desired performance from a mixed-flow pump [1, 2].

Recently, studies about fluid machinery designing using optimization technique and CFD are actively carried out. Especially, researches on pump hydraulic design for improve performance are actively being carried out. Heo et al. have analyzed the flow-field of fluid machinery by using CFD and conducted a study of performance improvement in fluid machinery based on the analysis result [3]. Kim et al. have studied optimal designing of impeller and volute in centrifugal pump by using design of experiment as well as CFD [4].

Virendra et al. analyzed varying performance of turbine according to the changes of shaft diameter by using CFD. Virendra et al. analyzed changing efficiency of turbine according to the changes of shaft diameter and suggested few methods to improve efficiency [5].

Wen et al. analyzed the performance of mixed-flow pump according to the changes of diffuser hub radius by using CFD and tests. The changes of total head and efficiency according to diffuser hub radius were analyzed and the results of CFD were verified through performance experiments [6].

In this study, the impeller shape of the inlet part according to the hub ratio was analyzed and the impeller was optimally

*Corresponding author. Tel.: +82 41 589 8337, Fax.: +82 41 589 8330
E-mail address: yschoi@kitch.re.kr
† Recommended by Associate Editor Won Gyu Shin

designed according to the hub ratio. For design optimization, the main design variables of impeller were designed using the Response surface method (RSM). The tendency of the impeller design variables according to the hub ratio was analyzed by using the optimally designed impeller shape. The impeller shape was designed from the tendency of the impeller design variables according to the hub ratio. Finally, the performance of the impeller shape was verified using numerical analysis.

2. Mixed-flow pump impeller design method

Impeller is very important component of mixed-flow pump and it changes kinetic energy of fluids into pressure energy. In impeller designing, blade shape and sweep angles can be expressed as meridional plane and front plane. Meridional plane and front plane is expressed as cylindrical coordinate.

In Fig. 1, (a) expresses meridional plane of impeller while (b) and (d) show front plane and the-dimensional shape of the impeller respectively. Meridional plane represents the size and blade shape of the impeller as well as the information of r and z of cylindrical coordinate. Front plane depicts sweep angle depending on circular arc of the impeller as well as the information of r and θ of cylindrical coordinate.

Although meridional and front plane represent blade shape and sweep angles, cylindrical coordinate provided from these planes also needs to be analyzed in order to understand blade angle distribution. Vane plane development can be expressed by using the information from the meridional and front plane of the impeller and one of its advantages is that blade angle distribution can easily be shown on it. In Fig. 1, (c) is two-dimensional plane of vane plane development [7, 8].

Designing of meridional plane and blade angle distribution is required in order to design impeller shape. The base meridional plane of impeller was designed by analyzing previous studies and data base while blade angle distribution was designed by using vane plane development. Design variables of meridional plane and vane plane development that controls impeller shape were identified in order to optimal designing of the impeller. Pump performance depending on the changes of design variables was analyzed by utilizing CFD while RSM was used in order to carry out optimal designing with improved pump performance. The performance of optimally designed impeller was verified using CFD and the result was compared with that of reference model. Table 1 shows the design specifications. Specific speed (rpm, m^3/min, m) of impeller from mixed-flow pump is 550.

Table 1. Design specifications.

Q [CMH]	Ht [m]	RPM
420	17.5	1780

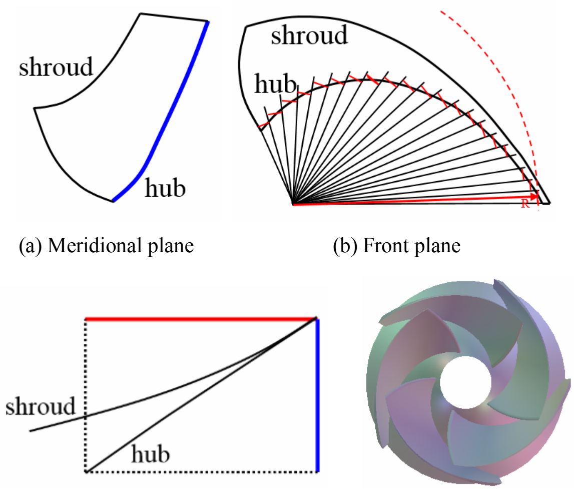

(a) Meridional plane (b) Front plane

(c) Vane plane development (d) 3D impeller shape

Fig. 1. Traditional design method of the impeller [7, 8].

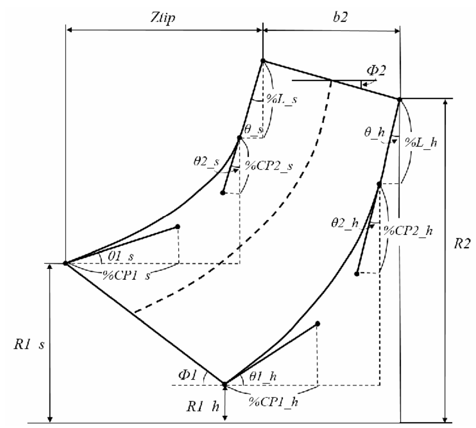

Fig. 2. Design variables for meridional plane [9].

2.1 Design variables in meridional plane

In order to design meridional plane which shows the information of impeller shape and size, design variables of meridional plane were defined as shown in Fig. 2.

Ordinary meridional plane is designed as arc type. However, making it arc type might not satisfy pump performance although the designing the curve of meridional plane can be simpler. Therefore, accurate definition of design variables for meridional plane is required to design meridional plane that satisfies performance.

In this study, Bezier curve was used for accurate designing of meridional plane. In Fig. 1, *R1* indicates the radius of inlet part and *R2* indicates the radius of exit part. *b2* is width of outlet part while *Ztip* indicates the length of axial direction between inlet and outlet of impeller shroud. *Phi1* is gradient of leading edge for impeller while *Phi2* is that of trailing edge for impeller. The curve on meridional plane was connected smoothly and bezier curve was used to smoothly connect inlet part and exit part of meridional plane. *θ1* is a gradient of inlet part and *θ2* is that of exit part on the curve of meridional plane. *%CP1* and *%CP2* are control points of inlet part and outlet part that control Bezier curve. *%L* indicates section of straight line from outlet part of impeller while θ indicates the gradient of straight lined section from the outlet part of impeller. Among design variables of meridional plane, h means hub while s indicates shroud [9].

2.2 Design variables in vane plane development

Design variables of vane plane development were defined as shown in Fig. 3 in order to design vane plane development that represents information regarding distribution of impeller blade angles.

Vane plane development provides information of impeller inlet and outlet angles as well as distribution of impeller blade angles and it makes it easier to control inlet and outlet angles along with distribution of blade angles. Therefore, if design variables of vane plane development are defined accurately, the distribution of blade angles as well as impeller inlet and outlet angles can be designed easily. Vane plane development was designed in a way where impeller inlet angle is connected to impeller outlet angle smoothly. Therefore, beta distribution is expressed as linear distribution.

In Fig. 3, inlet angle of impeller was defined to be $\beta 1$ while exit angle was defined to be $\beta 2$. $\%\beta 1$ and $\%\beta 2$ were defined to represent the identical sections from inlet and outlet angles and $\%\beta 1$ and $\%\beta 2$ were expressed as percentage of the length of meridional plane. $\sum R\_d\theta$, which is Y axis of vane plane development, is a sum of arc length while X axis $\sum dM$ is a sum of meridional plane length. hub, mid-span, and shroud were defined as h, m and s, respectively in vane plane development [9].

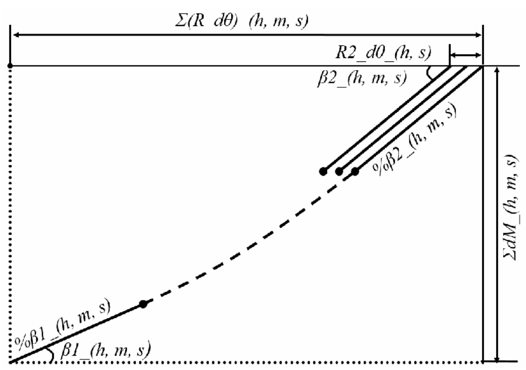

Fig. 3. Design variables for vane plane development [9].

3. Mixed-flow pump impeller design according to hub ratio

Shaft diameter is calculated using shaft power and rotational speed. Shaft diameter increases when flow rate increases at the same specific speed. Pump designing is difficult for a fixed hub ratio when flow rate increases at the same specific speed. The optimally designed Ns550 mixed-flow pump in a previous study was used as the reference model. Each hub ratio in the reference model was increased by 5 % from the impeller diameter. The hub ratio indicates the ratio of the impeller inlet hub diameter and outlet shroud diameter. Fig. 4 shows the impeller meridional plane depending on the hub ratio. Fig. 4 indicates that as the hub diameter increased, the inlet shape of the meridional plane varied according to the following conditions:

(1) The inlet area of the meridional plane was designed to be identical to that of the reference model.

(2) When the hub diameter of the inlet part increased, the axial positions of the inlet hub remained unchanged.

(3) The gradients of the impeller inlet part were identical.

(4) When the hub diameter of the inlet part increased, the shroud diameter of the inlet part and the axial position of the inlet shroud that satisfied (1)~(3) were selected.

The optimum impeller design was carried out on the meridional plane, the hub ratio of which is 0.15. $\theta 1\_h$, which is the

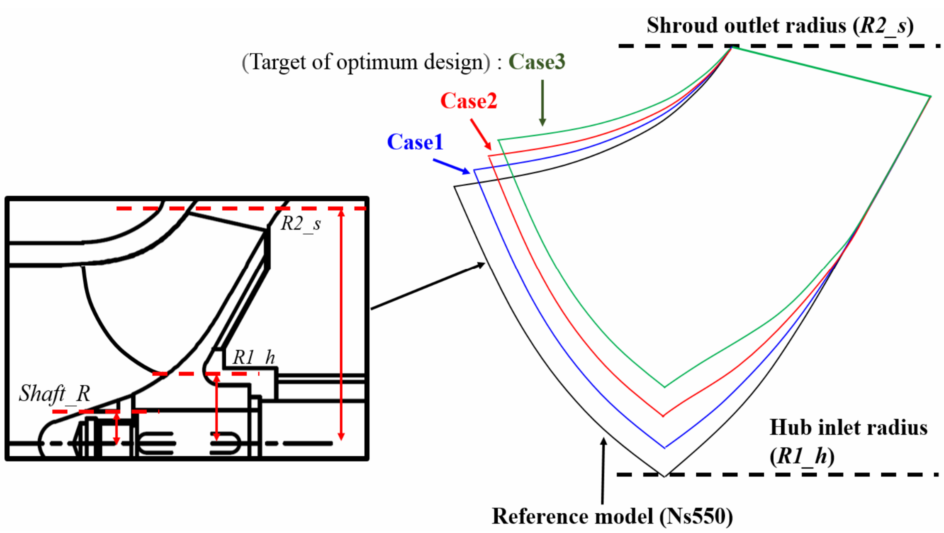

Fig. 4. Comparison of meridional plane for hub ratios.

Table 2. Specifications of measurement devices.

Measurement device	Range	Uncertainty
Torque meter	0~200 Nm	±0.2 %
Flow meter	0~900 m^3/hr	±0.2 %
Rotational sensor	0~20000 r/min	±0.02 %
Absolute pressure transducer	0~200 kPa	±0.25 %
Differential pressure transducer	0~500 kPa	±0.2 %

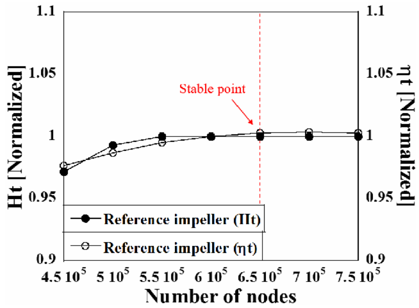

Fig. 5. Result of grid dependency test.

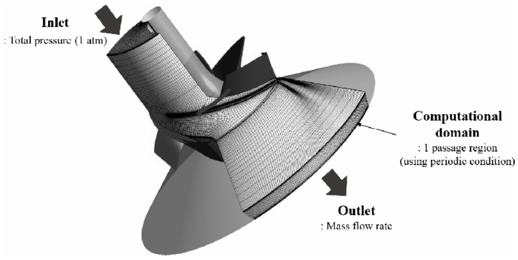

Fig. 6. Boundary conditions & grid system for impeller calculation.

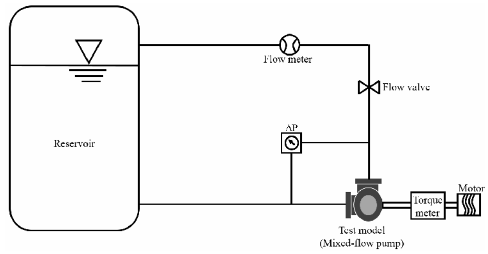

Fig. 7. Schematic diagram of experimental apparatus for a mixed-flow pump [16].

incline angle of the hub meridional curve in the inlet part, and *iβ1_h* and *iβ1_s*, which are the incidence angles of the hub and shroud, respectively, were chosen as the impeller design variables.

4. Numerical analysis method

Commercial program ANSYS CFX-16.0Ver. was utilized for flow-field analysis of internal impeller as well as verification of performance for impeller.

Structured grid was generated by using turbo-grid for internal flow passage of the impeller. The impeller has 5 blades and they have identical blade shape. Therefore, numerical analysis was carried out using periodic condition on only one blade domain. After the mesh test, 650000 grids were used for the impeller analysis. Fig. 5 shows the result of grid test on the impeller.

Atmospheric pressure was applied to impeller inlet part while mass flow-rate was given to outlet part. The shape of numerical analysis for the impeller as well as boundary condition are shown in Fig. 6. Working fluid of impeller is water [10-12]. RANS (Reynolds average Navier-Stokes) equation was used for turbulent flow analysis for incompressible fluid as water is incompressible flow-field. SST (Shear stress transport) k-w model was used as turbulent model which makes it possible to predict flow separation of flow-field for the impeller [13-15].

5. Validation of reference model

Reference model is an optimally designed shape that has been developed through previous studies. The reference model was optimally designed by applying CFD and optimization method on impeller design variables (Meridional plane and vane plane development). The performance of optimally designed reference model has been verified with CFD and performance test. The experiment and CFD results were normalized by the CFD results of design-flow rate for the reference model.

Fig. 7 shows an experiment apparatus for pump performance test. The pump performance test consists of a reservoir, a pressure gauge, an electromagnetic flowmeter, a flow control valve and a torque meter. The electrical motor that was connected to test pump was controlled by using an inverter. The range and uncertainty of main measurement device from the experiment apparatus are shown in Table 2 [16].

In order to verify the performance of reference model, the numerical analysis results and experimental results were compared and analyzed. The performance curve of the reference model was verified by using CFD and experiment. Fig. 8 is the comparison of CFD and experimental result of the reference model.

Fig. 8(a) is the comparison of total head curve from numerical analysis and experimental result while Fig. 8(b) is the comparison of total efficiency curve. Diffuser loss is confirmed when the results of impeller CFD and the result of impeller and diffuser CFD are analyzed. The result of performance experiment for the reference model includes impeller and diffuser. In Fig. 8, CFD result of the impeller and diffuser is similar to the performance curve of performance test result. However, the test results were smaller than the numerical results. That is because factors such as bell mouth effect, tip clearance effect, disk friction loss, and leakage loss are not included in the numerical analysis results. The tendencies of performance curves are similar between the numerical analysis results and experimental results from the reference model.

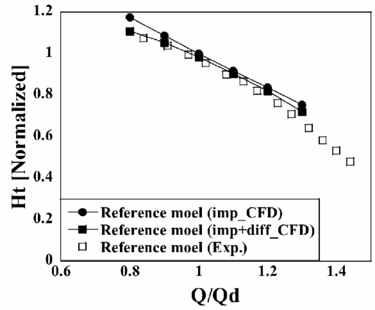

(a) Performance evaluation of the total head

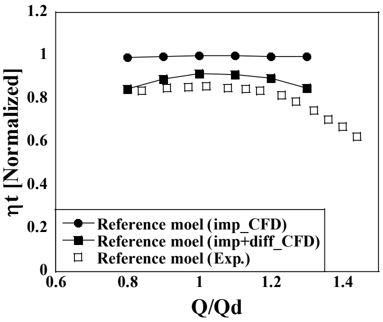

(b) Performance evaluation of the total efficiency

Fig. 8. Comparative analysis of the performance evaluation for reference model (Experiment vs. numerical analysis).

6. Optimally designed impeller

The optimum impeller design was carried out using Response surface method (RSM). The purpose of RSM is to find the optimal conditions for a design variable that could optimize the response variable [17, 18]. In RSM, the objective functions are required in order to analyze the performance depending on the changes of design variables. Objective functions were defined on total head curve and total efficiency curve which are performance curves of a pump. Fig. 9 shows total head curve and total efficiency curve that defined objective functions. A pump has its total head fixed at design specification and designed to have high efficiency. Therefore, the objective functions were defined to be total head and total efficiency at design flow rate. Total head and total efficiency are calculated by Eqs. (1) and (2).

$$Ht = \frac{Pt\_out - Pt\_in}{\rho g} \tag{1}$$

$$\eta t = \frac{(Pt\_out - Pt\_in)\times Q}{\tau \times \omega}. \tag{2}$$

In Eq. (1), *Pt_out* indicates the outlet total pressure and *Pt_in* indicates the Inlet total pressure. ρ is the density while g indicates the acceleration of gravity. In Eq. (2), Q is the flow rate and τ is the torque. ω is the Angular velocity.

The changes of total head and total efficiency depending on the changes of design variables were analyzed. Optimum design was carried out based on the analysis result. Proper experimental conditions need to be selected as design variables for optimum design. Experimental conditions of design variables were selected by utilizing central composite [19-21].

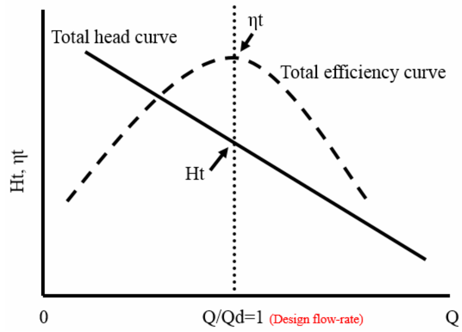

Fig. 9. Objective functions (Total head, total efficiency).

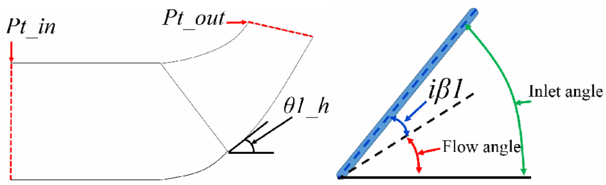

(a) Meridional design variable (b) Blade angle design variable

Fig. 10. Impeller design variables for RSM.

As for the optimum design of impeller, *iβ1_h*, *iβ1_s* and *θ1_h* were selected to be main design variables using RSM. *iβ1_h* and *iβ1_s* are incidence angles of hub and shroud respectively. Incidence angle means the difference of inlet angle and flow angle. *θ1_h* means gradient of inlet part of hub curve on meridional plane. Fig. 10 shows main design variables for optimum design.

As for optimum design of impeller, regression analysis was used for response optimization of design variables. Regression analysis is numerical anticipation of mathematical shape in order to analyze association between design variables and objective functions. Curvilinear regression analysis is a type of regression analysis where the relationship between design variables and objective functions is assumed to be curved. Regression analysis is presented in Eq. (3).

$$\hat{Y} = \widehat{\beta_0} + \widehat{\beta_1} \times X_1 + \widehat{\beta_2} \times X_2^{\ 2} + \cdots + \widehat{\beta_n} \times X_n^{\ n}. \tag{3}$$

X indicates the design variables and $\hat{\beta}$ is regression coefficient. $\hat{Y}$ is established by regression analysis. Here, the standard error of regression is less than 5 %. Hence, the accuracy of the curvilinear regression analysis is superior in this study.

Optimum design of the impeller was carried out on the meridional plane, as shown by Case 3 in Fig. 4. The hub ratio in Case 3 is 0.15. A main effects plot was used in order to analyze the tendencies of response variables according to the impeller design variables. Fig. 11 shows the optimization flowchart for optimum design of impeller.

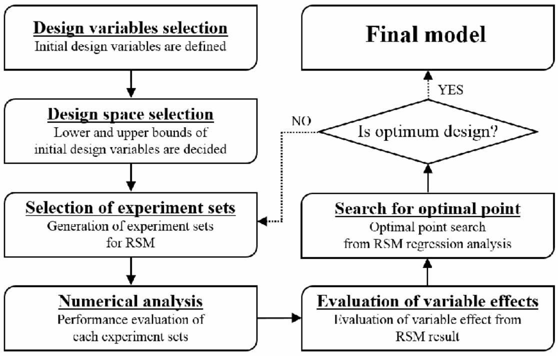

Fig. 11. Optimization flow chart.

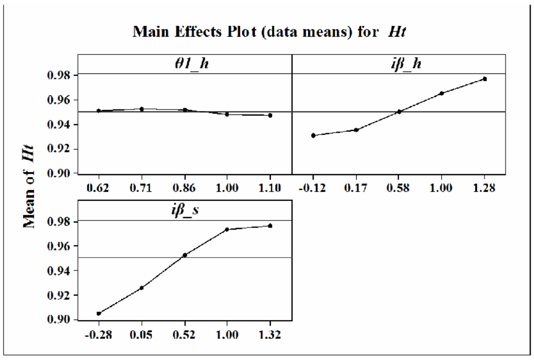

Fig. 12. Main effects plot for total head.

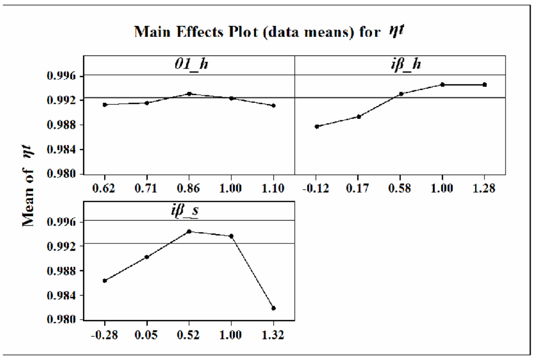

Fig. 13. Main effects plot for total efficiency.

Figs. 12 and 13 show the main effects plots. In Fig. 12, the total head increases as *iβ1_h* and *iβ1_s* increase. However, *θ1_h* tends to be the highest total head at 0.71. In Fig. 13, the total efficiency is highest when *θ1_h* is about 0.85, while it is highest at *iβ1_h* and *iβ1_s* values of 1.0 and 0.52, respectively. The optimum impeller design was carried out such that the efficiency could be improved since the total head according to changes in the design variables of impeller satisfies the design specifications.

When main effects flot is analyzed, the tendencies of total head and total efficiency depending on the changes of design variables can be predicted. In order to numerically express total head and total efficiency depending on the changes of design variables, regression analysis shown in Eq. (3) was used. Optimal condition of design variables can be found if total head and total efficiency are digitized according to the changes of design variables. Objective function for optimum design was set to be maximum efficiency. Total head is influenced significantly by the shape of impeller exit part. The shape of impeller exit part according to hub ratio is same as the reference model. Therefore, total head was excluded from the objective function.

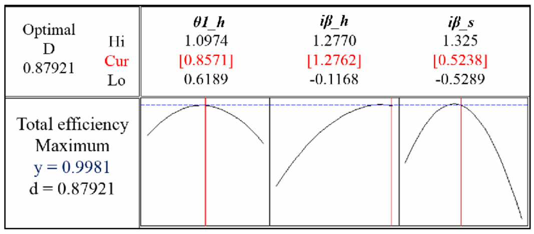

Fig. 14. Plot for response optimization.

The plot of response optimization shown in Fig. 14 was drawn using RSM. With regard to the result of response optimization, the total efficiency was predicted to be 0.9981 when *θ1_h* = 0.86, *iβ1_h* = 1.28 and *iβ1_s* = 0.52. This impeller performance result was verified using numerical analysis [22]. The design and objective functions were normalized by the design flow rate of the reference model.

7. Tendency analysis of impeller design variables according to hub ratio

The tendency of the design variables according to changes in the inlet part hub diameter was analyzed using the reference model and the Case 3 shape constructed on the basis of previous studies. Fig. 15 shows the tendencies of *θ1_h*, *iβ1_h* and *iβ1_s*. The hub ratio in each case improved by a value of 0.05 from the reference model hub ratio, which was 0. The hub ratio in Cases 1-3 were 0.05, 0.1 and 0.15, respectively. In Figs. 15(a) and (c), *θ1_h* and *iβ1_s* decrease as the hub ratio increases. However, in Fig. 15(b), *iβ1_h* increases as the hub ratio increases. By analyzing the tendencies of the design variables in Fig. 15, we can observe that the tendencies of *θ1_h* and *iβ1_s* are opposite to that of *iβ1_h*.

The equations of tendency for *θ1_h*, *iβ1_h* and *iβ1_s* are as follows, respectively:

$$\theta 1\_h = 1 - 0.95 \times \text{hub ratio} \quad (4)$$

$$i\beta 1\_h = 1 + 1.85 \times \text{hub ratio} \quad (5)$$

$$i\beta 1\_s = 1 - 3.17 \times \text{hub ratio}\,. \quad (6)$$

The impeller shape is designed using the design variable tendencies shown in Fig. 15.

The designed impeller shape is shown in Fig. 16. In Fig. 16, Cases 1 and 2 are designed using the design variable tendencies shown in Fig. 15. An optimally designed impeller shape from a previous study was chosen to be the reference model. Case 3 shows the optimally designed shape with a hub ratio of

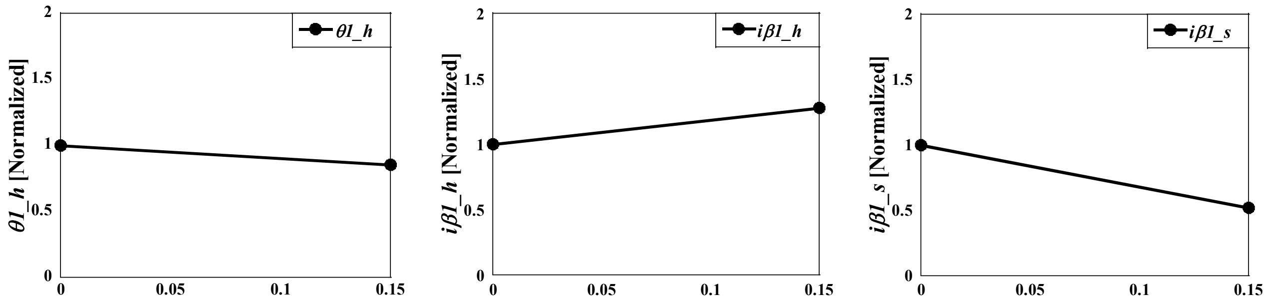

(a) $\theta 1\_h$ (b) $i\beta 1\_h$ (c) $i\beta 1\_s$

Fig. 15. Tendency of design variables.

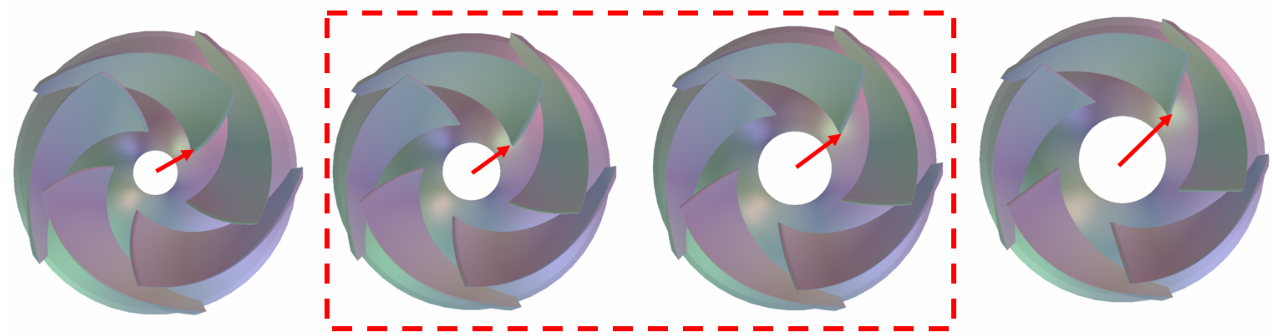

(a) Reference model (b) Case 1 (c) Case 2 (d) Case 3

Fig. 16. Comparison of three-dimensional geometry impeller.

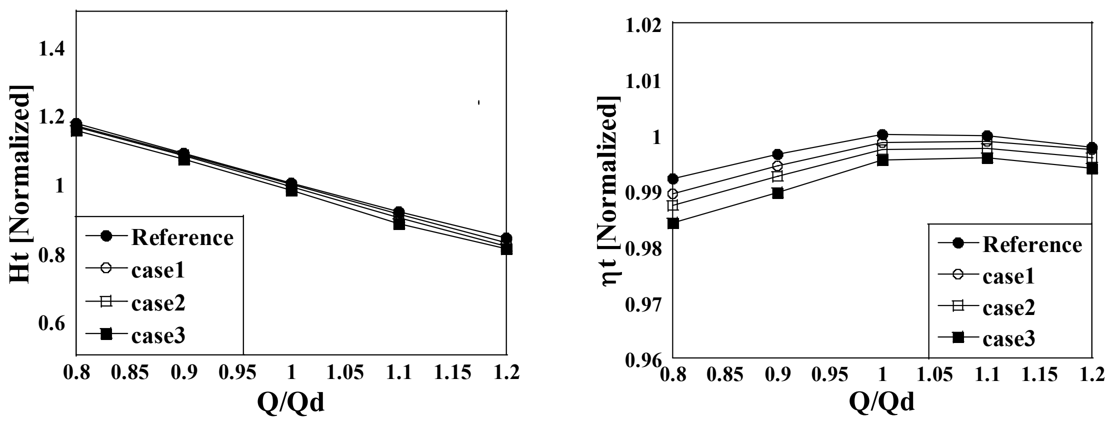

(a) Total head curve (b) Total efficiency curve

Fig. 17. Comparison of total head and total efficiency curve.

0.15. Fig. 16 shows a comparison of the impeller shapes according to changes in the hub ratio. Impeller inlet shapes are different depending on the hub ratio. The other design variables of impeller were fixed to be design variables of the reference model.

8. Analyses of numerical analysis results according to hub ratio

Fig. 17 shows a comparison between the total head and total efficiency curves for the impeller depending on the hub ratio. The impeller designed on the basis of the design variable tendencies was subjected to performance verification conducted using numerical analysis [23]. In Fig. 17(a), the tendencies of the total head curves depending on the impeller shape are similar. Similarly, the total heads at the design flow rate are almost identical. In Fig. 17(b), the tendencies of the total efficiency curves according to the impeller shape are similar, and the maximum efficiency is expected at the design flow rate. The total efficiency in Cases 1 and 2, which are based on the design variable tendencies, is lower than that of the reference model at the design flow rate. However, the total efficiency in

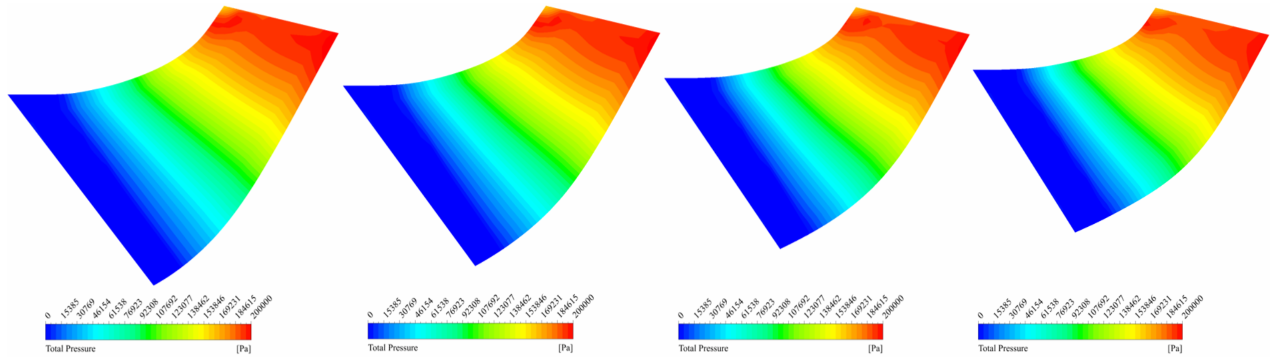

(a) Reference model (b) Case 1 (c) Case 2 (d) Case 3

Fig. 18. Comparison of the total pressure contour on the meridional plane.

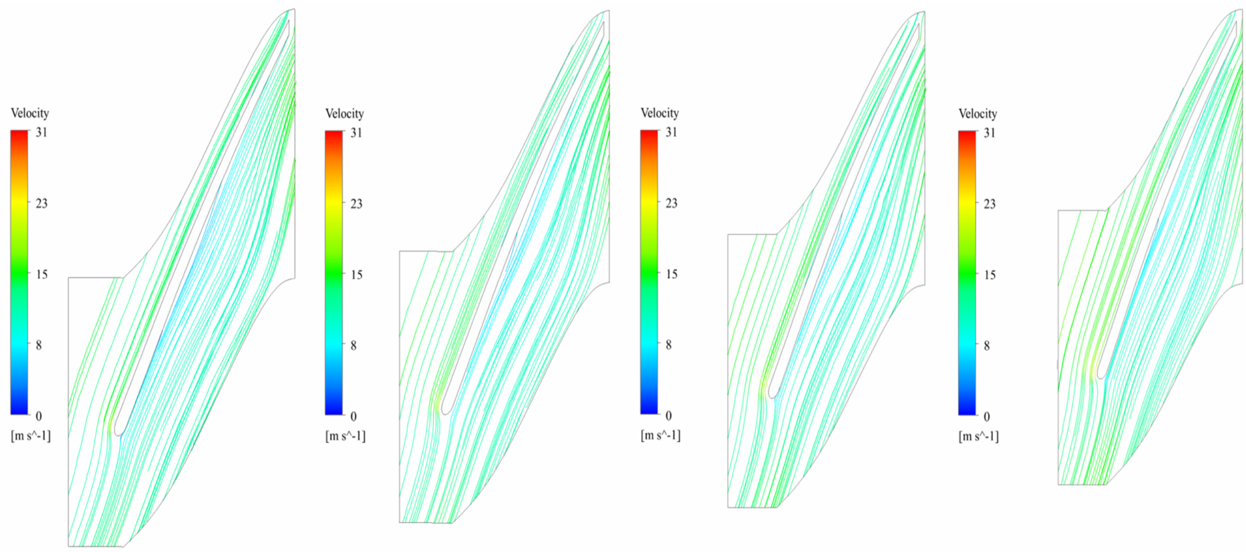

(a) Reference model (b) Case 1 (c) Case 2 (d) Case 3

Fig. 19. Comparison of the streamline on the blade to blade at mid-span.

these cases is higher than that in the optimally designed Case 3 for which the hub ratio is 0.15.

Fig. 18 compares total pressure contour of each impeller shape. From total pressure distribution of each shape, it is obvious that the tendencies of total pressure distribution are very similar. That is because the loss of total pressure is minuscule with similar total head curves according to changing hub ratio as it is seen from the total head curves in Fig. 17(a).

Fig. 19 compares streamline of each impeller shape. As shown in Fig. 19, the streamline of fluid flow for each shape is very smoothly. That is also due to the fact that the loss of total efficiency is minimum according to the changes of hub ratio as it is seen from the total efficiency curves in Fig. 17(b).

It can be said that the performance of the impeller with a shape that was designed using the design variable tendencies depending on changes in the hub ratio is almost identical to that of impeller with the optimally designed shape. Moreover, this impeller could satisfy the design specifications at the same specific speed.

9. Conclusions

In this study, the impeller shape and performance according to the hub ratio at an unchanged specific speed were analyzed. The impeller was designed on the basis of design variable tendencies according to the hub ratio. The following conclusions have been drawn from this research:

(1) The result of performance test on the reference model with numerical analysis can be credited because the tendencies of performance curves are similar when numerical and experimental result of reference model are compared and analyzed.

(2) The impeller shape can be designed according to the hub ratio in the same impeller area, and the optimum design can be determined using design variables of the impeller inlet part.

(3) The tendency of design variables can be analyzed according to the hub ratio, and the impeller shape depending on the various hub ratios can be designed on the basis of the design variable tendencies.

(4) The total head curve for the impeller, which is con-

structed using the design variable tendencies, is expected to be almost identical to that for the impeller with the optimally designed shape.

(5) The total efficiency curve for the impeller, which was constructed using the design variable tendencies, is expected to be almost identical to that for the impeller with the optimally designed shape. Further, the total efficiency is highest at the design flow rate.

(6) The impeller shape that satisfies the design specifications could be designed on the basis of design variable tendencies according to changes in the hub ratio.

(7) The hub ratio that is related to shaft diameter is very important when designing impeller of mixed flow pump. Performance analysis depending on hub ratio is important as the performance of mixed-flow pump varies according to hub ratio. Impeller shape that satisfies pump performance from various shaft diameters can be designed if pump performance depending on hub ratio is analyzed.

Acknowledgements

This research was supported by a grant (No. 10044860) from the Korea Institute of Industrial Technology Evaluation and Planning (ITEP) that is funded by the Ministry of Science, ICT, and Future Planning.

Nomenclature

CFD : Computational fluid dynamics
RSM : Response surface method
Ht : Total head
M : Meridional length
N : Rotational speed
Ns : Specific speed
Pt_in : Inlet total pressure
Pt_out : Outlet total pressure
Q : Flow rate
Qd : Design flow rate
R1 : Radius
R2 : Radius of diffuser inlet
Ztip : Axial direction from inlet/outlet parts of the shroud
g : Acceleration of gravity
h : Hub
m : Mid-span
s : Shroud
Φ1 : Inclined angle of the leading edge
Φ2 : Inclined angle of the trailing edge
β1 : Inlet angle of impeller
iβ1 : Incidence angle
θ1 : Inlet angle from meridional curve
θ2 : Outlet angle from meridional curve
%L : Straight line from outlet part
%CP1 : Control points of inlet part
%CP2 : Control points of outlet part
%β1 : Portion of same inlet blade angle
%β2 : Portion of same outlet blade angle
ρ : Density
ω : Angular velocity
τ : Torque

References

[1] K. Imaichi, Y. Murakami, H. Tsurusaki and K. R. Cho, *The basis of pump design*, Daiyoungsa (2002) 307-375.

[2] J. Stepanoff, *Centrifugal and axial flow pumps*, John Wiley & Sons (1957) 144-150.

[3] M. W. Heo, K. Kim, J. H. Kim and Y. S. Choi, High efficiency design of a mixed-flow pump using a surrogate model, *Journal of Mechanical Science and Technology*, 30 (2) (2016) 541-547.

[4] J. H. Kim, H. C. Lee, J. H. Kim, S. Kim, J. Y. Yoon and Y. S. Choi, Design techniques to improve the performance of a centrifugal pump using CFD, *Journal of Mechanical Science and Technology,* 29 (1) (2015) 215-225.

[5] V. K. Yadav and S. K. Singal, Performance analysis of cross-flow turbine: Variation in shaft diameter, development of water resources in India, *Water Science and Technology Library*, 75 (2017) 487-497.

[6] W. P. Zhang, F. P. Tang, S. Y Zhou, Y. Xia, H. Y. Liu and C. H. Wu, Mixed-flow pump hydraulic analysis under different hub radius of guide vane, *The 14th Asian International Conference on Fluid Machinery* (2017) AICFM14-217.

[7] S. Kim, Y. S. Choi, K. Y. Lee and J. Y. Yoon, Design optimization of centrifugal pump impellers in a fixed meridional geometry using DOE, *International J of Fluid Machinery and Systems*, 2 (2) (2009) 172-178.

[8] S. Kim, Y. S. Choi, K. Y. Lee and J. H. Kim, Design optimization of mixed-flow pump in a fixed meridional geometry using DOE, *International Journal of Fluid Machinery and Systems,* 4 (1) (2011) 14-24.

[9] S. Kim, K. Y. Lee, J. H. Kim and Y. S. Choi, A numerical study on the improvement of suction performance and hydraulic efficiency for a mixed-flow pump impeller, *Mathematical Problems in Engineering,* 2014 (269483) (2014) 17.

[10] K. Y. Kim and S. J. Seo, Shape optimization of forward-curved-blade centrifugal fan with Navier-Stokes analysis, *Journal of Fluids Engineering*, 126 (5) (2004) 735-742.

[11] J. H. Kim, J. W. Kim and K. Y. Kim, Axial-flow ventilation fan design through multi-objective optimization to enhance aerodynamic performance, *ASME Journal of Fluid Engineering*, 133 (10) (2011) 101101.

[12] ANSYS Inc., Boundary conditions : Interface., *User manual for ANSYS CFX Pre version 13.0* (2012).

[13] J. H. Kim, B. M. Cho, S. Kim, J. W. Kim, J. W. Suh, Y. S. Choi, T. Kanemoto and J. H. Kim, Design technique to improve the energy efficiency of a counter-rotating type pump-turbine, *Renewable Energy*, 101 (2017) 647-659.

[14] G. Y. Wang, Y. Huo, B. Zhang, X. B. Li and Z. Y. Yu, Evaluation of turbulence models for predicting the performance of an axial-flow pump, *Trans. Beijing Inst. Technol.,* 4 (2009) 8.

[15] H. S. Shim and K. Y. Kim, Numerical investigation on hydrodynamic characteristics of a centrifugal pump with a double volute at off-design conditions, *International J of Fluid Machinery and Systems*, 10 (2017) 218-226.
[16] *ANSI/HI 1.6*, American national standard for centrifugal pump tests, Hydraulic Institute, USA (2000).
[17] X. Suna, S. Kim, S. D. Yang, H. S. Kim and J. Y. Yoon, Multi-objective optimization of a stairmand cyclone separator using response surface methodology and computational fluid dynamics, *Powder Technology*, 320 (2017) 51-65.
[18] U. H. Jung, J. H. Kim, J. H. Kim, C. H. Park, S. O. Jun and Y. S. Choi, Optimum design of diffuser in a small high-speed centrifugal fan using CFD & DOE, *Journal of Mechanical Science and Technology*, 30 (3) (2016) 1171-1184.
[19] U. H. Jung, Y. S. Choi and K. Y. Lee, Optimum design of volute configuration in a sirocco fan using CFD and DOE, *International Journal of Air-Conditioning and Refrigeration,* 17 (2) (2007) 68-73.
[20] C. R. Hick and K. V. Turner, *Fundamental concepts in the design of experiments*, Fifth Edition, Oxford University Press, New York (1999) 239-267.
[21] R. H. Myers and D. C. Montgomery, *Response surface methodology: Process and process and product optimization using designed experiments*, Second Edition, Wiley Interscience Publication (2002) 85-143.
[22] J. H. Kim, J. H. Kim, J. Y. Yoon, Y. S. Choi and S. H. Yang, Application of multi objective optimization techniques to improve the aerodynamic performance of a tunnel ventilation jet fan, *Proceedings of The Institution of Mechanical Engineers, Part C-Journal of Mechanical Engineering Science,* 229 (1) (2015) 91-105.
[23] J. H. Kim, H. C. Lee, J. H. Kim, Y. S. Choi, J. Y. Yoon, I. S. Yoo and W. C. Choi, Improvement of hydrodynamic performance of a multiphase pump using design of experiment techniques, *Journal of Fluids Engineering - Transactions of The ASME,* 137 (8) (2015) 081301.

Sung Kim received his B.S. and M.S. degrees from the Korea University of Technology and Education (KOREA TECH) and Hanyang University, Korea, in 2006 and 2009, respectively. He is currently a Researcher in the Korea Institute of Industrial Technology (KITECH). His research interests are designs of turbomachinery, numerical analyses, optimization techniques, and experimental tests.

Ung-Been Jeong received his B.S. and M.S. degrees from the Hanyang University, Korea, in 2014 and 2017. His research interests are designs of turbomachinery, numerical analyses, optimization techniques, and experimental tests.

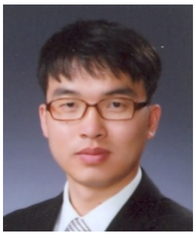

Kyoung-Yong Lee received his B.S. degree from the Korea University of Technology and Education (KOREA TECH) in 2002, and his M.S. and Ph.D. in Mechanical Engineering at the same university in 2004 and 2017, respectively. He has been a Senior Researcher in Thermal & Fluid System R&D Group, at Korea Institute of Industrial Technology (KITECH), Korea. His research interests are designs of turbomachinery, numerical analyses, system loss analyses, and experimental tests.

Jin-Hyuk Kim received his Ph.D. degree in Thermodynamics and Fluid Mechanics at Inha University, Korea, in 2013. He was a postdoctoral researcher in Faculty of Engineering at Kyushu Institute of Technology, Japan, in 2013. He is currently a Senior Researcher at Korea Institute of Industrial Technology (KITECH) and an Assistant Professor at University of Science and Technology (UST), Korea. His research interests are turbo machinery (Fans, compressors, pumps, turbines, and pump-turbines) designs and developments; steady and unsteady numerical analyses; optimization methods; flow measurements and experimental techniques.

Joon-Yong Yoon received his B.S. and M.S. degrees from the Hanyang University and Ph.D. degree from the Univ. of Iowa in mechanical engineering. He is a Professor of mechanical engineering at the Hanyang University. His research areas are CFD for applications, renewable energy, MEMS and flow control.

Young-Seok Choi received his B.S. degree from Seoul National University in 1988, and his M.S. and Ph.D. in Mechanical Engineering at the same university in 1990 and 1996, respectively. He is currently a Principal Researcher in Korea Institute of Industrial Technology (KITECH) and a Professor at University of Science and Technology (UST). His research interests are in computational fluid dynamics and design optimization of turbomachinery.